

Benzalhydantoin Derivative-Based Inhibitors of Eight Receptor Tyrosine Kinases: Synthesis, *in-vitro*, and *in-silico* Study

(Perencanaan Berasaskan Terbitan Benzalhidantoin bagi Lapan Reseptor Tيروسina Kinase: Kajian Sintesis, *in-vitro* dan *in-silico*)

MUHAMMAD NAUFAL¹, IKA WIANI HIDAYAT¹, ELVIRA HERMAWATI², YANA MAOLANA SYAH² & JAMALUDIN AL-ANSHORI^{1,*}

¹*Department of Chemistry, Faculty of Mathematics and Natural Sciences, Universitas Padjadjaran, Jl. Raya Bandung-Sumedang km.21, Jatinangor, 45363, Indonesia*

²*Division of Organic Chemistry, Faculty of Mathematics and Natural Sciences, Institut Teknologi Bandung, Jl. Ganesha 10, Bandung 40132, Indonesia*

Received: 11 July 2024/Accepted: 31 October 2024

ABSTRACT

Some hydantoin derivatives have been explored for their potential as anticancer agents by inhibiting receptor tyrosine kinases (RTKs). Benzalhydantoin derivatives were obtained from a two-step reaction: condensation and alkylation reaction. The benzalhydantoin activities were obtained from the enzymatic assay, while the molecular interaction was simulated with molecular docking. Five known compounds (**5-9**) and two new benzalhydantoin derivatives **10-11** have been synthesized from the appropriate precursors with 4-71% yields. The structures of the compounds were determined mainly by NMR and mass spectral data. From the chemical shift of the H-7', the configuration of the products **5**, **7**, **9-11** were determined as *Z*-isomer, while **6** and **8** were defined as *E*-isomer. A bioassay of the seven derivatives at 10 μ M against eight receptor tyrosine kinases (EGFR, HER2, HER4, IGF1R, InsR, VEGFR-2, and PDGFR- α and - β) showed that **8**: (*Z*)-5-(4'-hydroxy-3'methoxybenzylidene)imidazolidine-2,4-dione and **10**: (*Z*)-5-(4'-methoxybenzylidene)imidazolidine-2,4-dione were moderately active against VEGFR-2, with inhibition of 46 and 56%, respectively. In addition, **8** was also active against PDGFR- α and - β , with a 57% inhibition. Further evaluation of **8** and **10** using AutoDock4 showed their binding energy interactions with VEGFR2 (PDB ID: 4AG8) around -6.96 and -7.32 kcal/mol, respectively. Thus, both compounds are potential candidates to be optimized further as inhibitors of angiogenesis blood vessel development.

Keywords: Anticancer; hydantoin; *N*-heterocyclic; PDGFR α and - β ; tyrosine kinase; VEGFR-2

ABSTRAK

Beberapa terbitan hidantoin telah diterokai potensinya sebagai agen antikanser dengan menghalang reseptor tirosina kinase (RTK). Terbitan benzalhidantoin diperolehi daripada tindak balas dua langkah: tindak balas pemeluwapan dan alkilasi. Aktiviti benzalhidantoin diperolehi daripada ujian enzim, manakala interaksi molekul disimulasikan dengan dok molekul. Lima sebatian yang diketahui (**5-9**) dan dua terbitan benzalhidantoin baharu **10-11** telah disintesis daripada prekursor yang sesuai dengan hasil 4-71%. Struktur sebatian ditentukan terutamanya oleh NMR dan data spektrum jisim. Daripada anjakan kimia H-7', konfigurasi produk **5**, **7**, **9-11** ditentukan sebagai isomer *Z*, manakala **6** dan **8** ditakrifkan sebagai isomer *E*. Bioasai daripada tujuh terbitan pada 10 μ M terhadap lapan reseptor tirosina kinase (EGFR, HER2, HER4, IGF1R, InsR, VEGFR-2 dan PDGFR- α dan - β) menunjukkan bahawa **8**: (*Z*)-5-(4'-hydroxy-3'methoxybenzylidene)imidazolidine-2,4-dione dan **10**: (*Z*)-5-(4'-methoxybenzylidene)imidazolidine-2,4-dione adalah sederhana aktif terhadap VEGFR-2, dengan perencanaan masing-masing 46 dan 56%. Di samping itu, **8** juga aktif terhadap PDGFR- α dan - β dengan perencanaan 57%. Penilaian lanjut **8** dan **10** menggunakan AutoDock4 menunjukkan interaksi tenaga pengikat mereka dengan VEGFR2 (PDB ID: 4AG8) masing-masing sekitar -6.96 dan -7.32 kcal/mol. Oleh itu, kedua-dua sebatian adalah calon yang berpotensi untuk dioptimumkan lagi sebagai perencat perkembangan saluran darah angiogenesis.

Kata kunci: Antikanser; hidantoin; *N*-heterosiklik; PDGFR α dan - β ; tirosine kinase; VEGFR-2

INTRODUCTION

In recent decades, receptor tyrosine kinases (RTKs) have been the target for treating cancerous diseases. These

enzymes phosphorylate the tyrosine residue of other proteins using the substrate ATP, which regulates cell proliferation, metabolism, and motility (Du & Lovly 2018).

In some cancer development, such as non-small cell lung (NSCL) and breast cancers, anomalous expression and/or dysfunction of RTK have been linked to the incidence of these diseases (Butti et al. 2018; Dong et al. 2019). There are about 52 RTKs in human, including EGFR, HER2, HER4 (epidermal growth factor receptor), IGF1R, InsR (insulin receptor), VEGFR-2 (vascular endothelial growth factor receptor 2), and PDGFR- α and - β (platelet-derived growth factor receptor). EGFR, HER2, and HER4 activation initiate downstream signal transduction cascades that lead to DNA synthesis and cell proliferation, while IGF1R and InsR are involved in glucose homeostasis (Metibemu et al. 2019; Sun et al. 2020). VEGFR-2 is the RTK that, upon activated by vascular endothelial cell growth factor (VEGF), is implicated with the early stage of angiogenesis (Peng et al. 2017). Meanwhile, PDGFR- α and - β , among others, are also involved in developing blood vessels (Horikawa et al. 2015). Thus, inhibitors of these RTKs are essential in finding anticancer agents.

Many researchers have exploited hydantoin (imidazolidine-2,4-dione, **1**) derivatives because of their potential as pharmaceutical agents (Konnert et al. 2017) (Figure 1). The reported biological properties of these compounds include the antagonist of leukocyte function-associated antigen-1 (LFA-1), a selective androgen receptor modulator (SARM), anticonvulsant, anti-androgen, kinase inhibitors, muscle relaxant, and antibacterial (Cho, Kim & Shin 2019; Jangir et al. 2022; Naufal et al. 2024). Almost all the compounds are produced by synthesis, and very few of them occur naturally and are reported from marine organisms. These compounds were

the hydantoin derivatives **2-4** isolated from Red Sea sponges *Laxosubrites* sp. (**2**) and *Hemimycale arabica* (**3-4**) (Mudit et al. 2009). Compounds **2-4** belong to the arylidenehydantoin class (Figure 1), which can be synthesized from **1** with the corresponding arylaldehyde using Knoevenagel-type condensation (Mudit et al. 2009). In addition, arylidenehydantoin analogs were reported to inhibit EGFR (Carmi et al. 2006; Cavazzoni et al. 2008) and c-Met (Sallam et al. 2014) kinases.

Previously, we reported some hydantoin derivatives' synthesis and antimicrobial properties (**5-9**) (Hidayat et al. 2017, 2016). In an ongoing endeavor to investigate the biological activities of 5-benzylidene-hydantoin, our conjectures proposed that 5-benzylidene-hydantoin shows three structural characteristics as Small Molecule Kinase Inhibitors (SMKIs). First, the hinge region of the kinase is where the five-membered heterocyclics frequently form a hydrogen bond. Secondly, benzylidene moiety is expected to fill the hydrophobic region of the kinase catalytic domain. Third, alkyl chains are expanded into the solvent-exposed area of the kinase (Figure 1). Hence, this paper reported the synthesis of two new compounds **10-11** and seven new biological properties of **5-11** as the inhibitor of eight RTKs, namely EGFR, HER2, HER4, IGF1R, InsR, VEGFR-2, and PDGFR- α and - β . Moreover, molecular docking was also performed on all derivatives using AutoDock4 to evaluate their binding energy and interactions with VEGFR2 (PDB ID: 4AG8), using axitinib as a reference compound. Finally, the potential structure design that perhaps exhibited better activities and more selective interactions against VEGFR-2 was predicted based on the bioinformatics data.

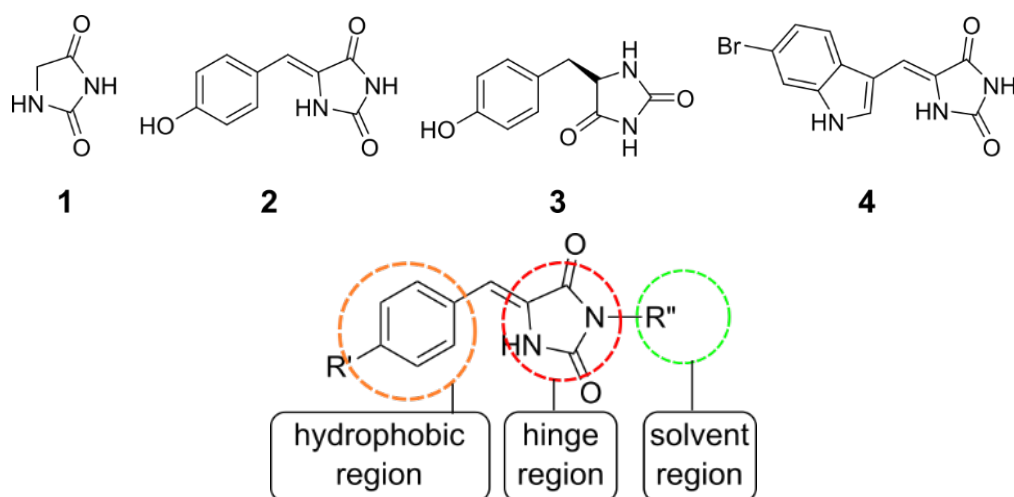


FIGURE 1. Hydantoin skeleton and natural arylidenehydantoin structures and structure rationalization of tyrosine kinase hydantoin-based inhibitors

MATERIAL AND METHODS

MATERIALS

Hydantoin, benzaldehydes, 1-chloropentane, and inorganic salts were purchased from Sigma-Aldrich Chemical Company, while the solvents were from Fischer Chemical Company. All solvents employed were of analytical grade and used without further purification. Thin-layer chromatography GF₂₅₄ and the silica gel G-60 for the column chromatography were obtained from Merck.

INSTRUMENTATION

The melting points were uncorrected and obtained using a Mettler Toledo MP50 Melting Point System. Infra-red spectra were obtained on Perkin Elmer Spectrum 100 FTIR spectrometers with potassium bromide (KBr) pellets. Exact masses were obtained using a high-resolution mass spectrometer (Waters Xevo QTOF HR-MS Lockspray). ¹H and ¹³C-NMR spectra were recorded on Agilent 500 MHz and 125 MHz spectrometers in CDCl₃ or DMSO-*d*₆ and referenced relative to the solvent peaks.

SYNTHESIS METHODS

The general procedure was done according to Hoffman and Wheeler's method (Raap et al. 1999). Briefly, hydantoins (50 mmol), benzaldehydes (50-150 mmol), and bases (anhydrous KOAc or NaOAc (Hidayat et al. 2017) or NH₄OAc (Reddy et al. 2010) were dissolved together in glacial AcOH (3 mL); subsequently Ac₂O (50 μL, 0.49 μmol) was added at r.t. and the mixture was heated to reflux temperature (110-115 °C) for 5-6 h. Reactions were monitored by thin-layer chromatography until all the aldehydes had reacted. Upon cooling, the mixture gave a precipitation that was collected and recrystallized from hot ethanol. The synthesis details and the spectroscopic data of the known compounds (**5-9**) were provided in Supplementary Material (available upon requests from the corresponding author).

(Z)-5-(4'-METHOXYBENZYLIDENE)IMIDAZOLIDINE-2,4-DIONE (**10**)

Hydantoins (5.0035 g, 50 mmol), 4-methoxybenzaldehyde (6.08 mL, 50 mmol), and anhydrous KOAc (50 mmol) were dissolved together in glacial AcOH (3 mL), then Ac₂O (50 μL, 0.49 μmol) was added at r.t. and the mixture warmed to reflux (115 °C, oil bath). Thin-layer chromatography was used to track the reactions until all the aldehydes had reacted. After it cooled and precipitated, the mixture produced a yellow solid and recrystallized from ethanol to give (Z)-5-(4'-methoxybenzylidene)imidazolidine-2,4-dione (**10**) as yellow needle (2.03 g, 20%) m.p. 248-249.9 °C. UV (MeOH) ν_{\max} nm (log ϵ): 335 (4.22); IR (KBr) ν_{\max} cm⁻¹: 3062, 2980, 2760, 1771-1680, 1601, 1432; ¹H NMR (500 MHz, DMSO-*d*₆) δ ppm: 11.15 (*br s*, NH-3), 10.42

(*br s*, NH-1), 7.59 (*d*, 8.8 Hz, H-2'/6'), 6.96 (*d*, 8.8 Hz, H-3'/5'), 6.39 (*s*, H-7'), 3.79 (*s*, OCH₃); ¹³C NMR (125 MHz, DMSO-*d*₆) δ ppm: 165.6 (C-4), 159.4 (C-4'), 155.6 (C-2), 131.1 (C-2'/6'), 126.1 (C-5), 125.4 (C-1'), 108.7 (C-7'), 55.3 (OCH₃); HR-ESI-MS *m/z*: [M+H]⁺ 219.0766 (calculated [M+H]⁺ for C₁₁H₁₀N₂O₃ 219.0764).

(Z)-3-PENTYL-5-(4'-METHOXYBENZYLIDENE)IMIDAZOLIDINE-2,4-DIONE (**11**)

Compound **10** (2.18 g, 10 mmol) was dissolved in 60 mL of DMF, and K₂CO₃ (5.9 g, 41 mmol) was added and stirred for 30 min. Then, 1-chloropentane (2.67 mL, 22 mmol) was added to the mixture, and the reaction was further stirred for 24 h. The reaction was quenched with 600 mL of water, extracted using EtOAc, washed with brine solution, and dried with Na₂SO₄. Crude was concentrated with a rotary evaporator and purified with column chromatography (Hexane:EtOAc (3:19 (v/v)) to give (Z)-3-pentyl-5-(4'-methoxybenzylidene)imidazolidine-2,4-dione (**11**) as white solids (192.3 mg, 17%) m.p. 155.5-156.4. UV (MeOH) λ_{\max} nm (log ϵ): 330 (4.01); IR (KBr) ν_{\max} cm⁻¹: 3264-3151, 3062, 2980, 2760, 1771-1680, 1601, 1432; ¹H NMR (500 MHz, CDCl₃) δ ppm: 8.34 (*br s*, NH-1), 7.40 (*d*, 8.8 Hz, H-2'/6'), 6.95 (*d*, 8.8 Hz, H-3'/5'), 6.70 (*s*, H-7'), 3.85 (*s*, OCH₃), 3.62 (*t*, 7.3 Hz, H₂-1''), 1.69 (*q*, 7.3 Hz, H₂-2''), 1.41-1.28 (4H, *m*, H₂-3''/4''), 0.90 (*t*, 7.0 Hz, H₃-5''); ¹³C NMR (125 MHz, CDCl₃) δ ppm: 164.1 (C-4), 160.2 (C-4'), 155.6 (C-2), 130.6 (C-2'/6'), 125.7 (C-1'), 124.6 (C-5), 114.7 (C-3'/5'), 111.9 (C-7'), 55.4 (OCH₃), 38.8 (C-1''), 28.9 (C-3''), 27.9 (C-2''), 22.3 (C-4''), 13.9 (C-5''); HR-ESI-MS *m/z*: [M+H]⁺ 289.1543 (calculated [M+H]⁺ for C₁₆H₂₀N₂O₃ 289.1547).

TYROSINE KINASE ASSAY

The method for the assay was done as previously described (Hennek et al. 2016; Zegzouti et al. 2009) and modified by Hermawati et al. (2020). In summary, the tested compound was prepared at 5% in DMSO and diluted using 4X kinase buffer (64.5 μL) and nuclease-free water (175 μL) to reach a final concentration of 10 μM. Additionally, each kinase stock was diluted with 2.5X reaction buffer (95 μL), and an 80 μM ATP solution (20 μL) was used to dilute the substrate/cofactor stock. The assay involved dispensing 1 μL of the tested compound, 2 μL of ATP/substrate, and 2 μL of kinase into each well of 384-well plates. The plates were then left to respond for an hour at a temperature between 22 and 25 °C. Next, 5 μL of ADP-Glo reagent was added, and the mixture was incubated for 40 min at 22-25 °C. After that, 10 μL of kinase detection reagent was added and incubated for 30 min. Following the process, the kinase activity was determined by measuring the luminescence. The well without the tested drug solution was the negative control (100% activity), and the well without the enzyme solution produced the background luminescence (0% activity). By deducting the background light from each and

every kinase reaction, the percentage of kinase activity was determined (Table 1). This assay utilized Erlotinib (10 μ M) as the positive control.

MOLECULAR DOCKING

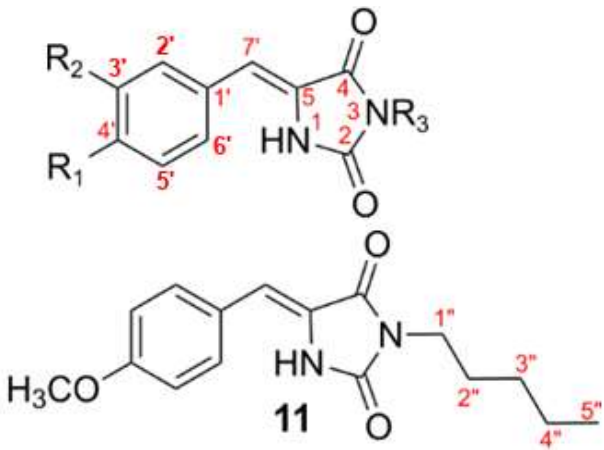
Before being subjected to molecular docking, ligands were modeled with GaussView, energy minimization was performed using the B3LYP method, and the 6-311++G(d,p) basis function was used throughout in Gaussian 09 revision D.01. Then, the output files were converted to PDB files. The receptor's structure was downloaded from a protein data bank, including axitinib (PDB ID code 4AG8) as a native ligand. Molecular docking validation was performed as follows (Morris et al. 2009; Yusuf et al. 2019). Water was stripped from a complex molecule (4AG8) since it is not involved in protein-ligand binding complexes. All hydrogens were added, non-polar hydrogens were merged, and ligands and receptor charges were calculated. After

adding hydrogens, axitinib was separated from the receptor structure (VEGFR2), and the input files were saved as PDBQT. Grid parameter file and gridbox were created to determine atom types and all residues involved in the receptor's binding site, and input files were saved as GPF. Docking parameter files were made to determine searching and docking parameters using the Lamarckian GA 4.2 method, and input files were saved as DPF. Grid calculation was performed using Autogrid 4.2, and molecular docking calculation was performed using Autodock 4.2. The results were analyzed using MGLTools, the 3D interactions were visualized using UCSF ChimeraX (Pettersen et al. 2020), and the 2D interactions were visualized using Biovia Discovery Studio.

RESULTS AND DISCUSSION

Compound **10** was obtained from hydantoin **1** and 4-methoxybenzaldehyde reaction using NaOAc as a base

TABLE 1. The tyrosine kinase activity of compounds **5-11** and erlotinib at concentration 10 μ M



	R ₁	R ₂	R ₃
5	H	H	H
6	OH	H	H
7	OH	H	CH ₃
8	OH	OCH ₃	H
9	OH	OCH ₃	CH ₃
10	OCH ₃	H	H
11	OCH ₃	H	C ₅ H ₉

Derivative	% Activity**							
	EGFR	HER2	HER4	IGF1R	InsR	VEGFR-2	PDGFR α	PDGFR β
5	83	114	91	96	76	120	93	84
6	88	80	121	94	91	66	88	79
7	85	88	85	105	90	79	83	66
8	78	95	83	100	101	46	57	57
9	82	98	78	104	102	121	86	73
10	78	86	124	103	101	56	83	79
11	96	110	119	106	114	104	98	103
Erlotinib	0	90	0	101	89	3	12	14

**strong: <20%, moderate: 20-60%, weak or not active: >60%

in acetic acid as a solvent. After recrystallization, the NH at position number 3 was alkylated by 1-chloropentane using K_2CO_3 in DMF (Figure 2). All the structures of reaction products **5-11** (Figure 2) were confirmed mainly by NMR and mass spectral data (Experimental and Supplementary Data - available upon requests from the corresponding author). The proton chemical shifts of H-7' appeared in the range of 6.35 – 6.70 ppm, suggesting that the benzalhydatoin derivatives **5**, **7**, **9-11** are in the *Z* configuration (6.4 – 6.7 ppm), while **6** and **8** are in the *E* configuration (6.3 ppm) (Thenmozhiyal, Wong & Chui 2004). Except for **5** (yield 71%), the yield for reactions between hydantoin and the corresponding oxygenated benzaldehydes, leading to the products **6-11**, was 4-20%. The results suggested that the presence of electron-donating substituents such as 4-OMe, 4-OH, and 4-OH, 3-OMe in the aryl part of benzaldehyde reduces the reaction yield due to the lowering of the electrophilic character of the aldehyde group. Similar observations are also reported with different heterocyclics (Akeng'a & Read 2007, 2005).

Compounds **5-11** and the positive control erlotinib (all at 10 μ M) were tested as the inhibitors of eight TKRs (EGFR, HER2, HER4, IGF1R, InsR, VEGFR-2, PDGFR α and - β) presented as % activity of the enzymes (Table 1). At least 100% activity means no inhibition, while 0% activity indicates complete enzyme inhibition. In this first screening, the potency of the compound was grouped into three categories, namely strong (% activity <20%), moderate (% activity 20-60%), and weak or inactive (% activity >60%). As shown in Table 1, erlotinib, which is known as a non-small cell lung cancer (NSCLC) drug and EGFR inhibitor, exhibited strong inhibitory effects against EGFR, HER4, VEGFR-2, PDGFR- α and PDGFR- β (% activity 0-14%) but was very weak or not active against HER2, IGF1R, and InsR (% activity 89-101%). None of the hydantoin derivatives exhibited strong inhibitory effects against the tested TKRs. However, compound **8** ((*Z*)-5-(4-hydroxy-3-methoxybenzylidene) imidazolidine-2,4-dione) showed moderate activity against VEGFR-2, PDGFR α , and PDGFR- β (% activity 46-57%), while **6** ((*Z*)-5-(4-hydroxybenzylidene) imidazolidine-2,4-dione) and **10** ((*Z*)-5-(3-methoxybenzylidene)imidazolidine-2,4-dione) have similar activities only against the VEGFR-2 (% activity 66 and 56%, respectively). The other tested

hydantoin derivatives **5**, **7**, and **9-11** were weak inhibitors or inactive to the tested TKRs. Thus, only **6**, **8**, and **10** showed selective activity as the inhibitor of VEGFR-2. Most kinases catalyze the transfer of phosphate groups from ATP to substrates, they share a highly conserved ATP-binding site. Many kinase inhibitors attach to the ATP-binding sites of numerous kinases, which can have off-target effects because they are made to compete with ATP at this binding site. It is challenging to attain high specificity because kinase ATP-binding pockets have structural similarities (Cohen 2002; Cohen, Cross & Jänne 2021). A small molecule kinase inhibitor that is selective is therefore very beneficial. Compounds **6**, **8**, and **10** showed moderate and selective inhibition towards VEGFR-2. This selectivity could be a foundation to develop kinase inhibitors based on hydantoin's skeleton. However, it would be more reasonable choice to design a prospective selective inhibitor with higher activity.

The results shown by **8** and **10** suggested that the additional oxygenated functional group, namely -OCH₃ in the aryl group for **8**, increased the inhibitory effects. Comparing the enzyme activities of **7**, **9**, and **11**, in which the NH-3 are alkylated, also suggested that the free NH-3 is an essential factor for inhibitory effects. It is also worth noting that the hydantoin derivatives **8** and **10** showed selective inhibitors against the regulation of angiogenesis (VEGFR-2) (**8** and **10**) and blood vessel development (**8** only) (PDGFR- α and PDGFR- β). These three TKRs are essential in the development of tumor-to-cancer states (Horikawa et al. 2015; Metibemu et al. 2019; Peng et al. 2017). Therefore, **8** and **10** can be regarded as promising lead compounds to be developed further as inhibitors of anticancer agents.

Molecular docking was performed towards **5-11** using AutoDock4 to evaluate its binding energy and interactions with VEGFR2 (PDB ID: 4AG8) along with axitinib as a reference compound. The crystal structure of the 4AG8 enzyme provides the most physiologically appropriate build of a target VEGFR-2 kinase, including phosphorylation state and regulatory domains, to fully clarify essential binding modalities and the resulting on-target potency and selectivity (McTigue et al. 2012). Axitinib is a selective VEGFR-2 inhibitor and a five-membered heterocyclic with an unsaturated double bond. Since 5-benzylidene-

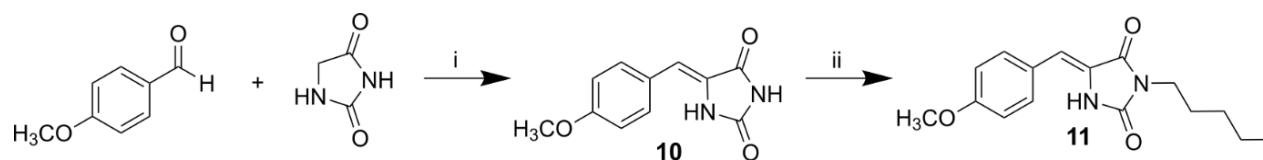


FIGURE 2. Synthesis scheme of compounds **10** and **11**. (i: NaOAc, AcOH, Ac₂O, 115 °C. 8 h. ii: K₂CO₃, DMF, r.t, 24 h)

hydantoin and axitinib have quite similar structural properties, axitinib is utilized as the reference chemical in this molecular docking experiment. Docking towards 4AG8 with axitinib as a native ligand was validated with an RMSD value of 1.11 Å. Axitinib exhibited a binding energy of -12.78 kcal/mol (Figure 3). The structures of all tested compounds (**5-11**) were structurally optimized using the B3LYP method (6-311++G(d,p) basis function) to achieve the most favorable geometric configurations. This method is widely used due to the balance of calculation accuracy and efficiency, validated and extensively benchmarked for neutral organic compounds containing C, H, N, and O atoms, and highly optimized in many quantum chemistry software packages (Tirado-Rives & Jorgensen 2008). Compounds **5-11** exhibited higher binding energy than axitinib, ranging from -6.47 to -7.94 kcal/mol (Table 2). Numerous retrospective studies have demonstrated that experimental binding affinity and docking scores frequently have weak correlations. This is because molecular docking generally uses sampling algorithms on rigid protein structures to reduce computational calculation cost and time.

Nonetheless, docking techniques are a great way to anticipate ligand binding positions by visually analyzing

the observed binding resemblance and examining hydrogen bonds and steric and hydrophobic interactions in contrast to crystal structure (Fischer et al. 2021; Wang et al. 2016). Hence, in this study, molecular docking calculation was performed to investigate compounds **5-11** binding poses and interactions. Three moderately active compounds (**6**, **8**, and **10**) in tyrosine kinase assay posed similarly among each other in the VEGFR-2 active pocket where hydantoin moiety resided in the hydrophobic pocket. Both amide fragments of hydantoin and axitinib formed hydrogen bonds with either Glu885 of the VEGFR-2 allosteric region or Asp1046 of the VEGFR-2's DFG motif. Hydroxyl and methoxy benzylidene moiety of **6**, **8**, and **10** formed an H-bond with Cys919 of VEGFR-2's hinge region (Figure 3). Adenine of ATP formed hydrogen bonds in the hinge region; by interacting with this region, 5-benzylidene-hydantoins can potentially bind competitively with ATP to block the kinase catalytic activity (Xing et al. 2015). DFG motif regulates active/inactive enzyme conformations. Maintaining interaction with the DFG motif could stabilize the inactive state, which is crucial for inhibiting VEGFR-2 kinase activity (Zhao et al. 2014).

Meanwhile, the methylated analogs (**7** and **9**), which have weaker inhibition, are reversely posed with

TABLE 2. Molecular docking of **5-11** against VEGFR-2 (PDB ID: 4AG8)

Compounds	Lowest Binding Energy (kcal/mol)	Binding interaction
5	-6.47	H-bond: Glu885, Asp1046. Hydrophobic interaction: Val848, Ala866, Leu840, Leu1035, Val899, Phe1047
6	-6.85	H-bond: Asp1046, Cys919. Hydrophobic interaction: Val848, Ala866, Leu840, Leu1035, Val899
7	-7.02	H-bond: Asp1046, Cys919. Hydrophobic interaction: Val848, Ala866, Leu840, Leu1035, Val899, Phe918
8	-6.96	H-bond: Asp1046, Cys919. Hydrophobic interaction: Val848, Ala866, Leu840, Leu1035, Val899, Cys1045
9	-7.25	H-bond: Cys919, Glu885. Hydrophobic interaction: Val848, Ala866, Leu840, Leu1035, Val899, Phe918, Cys1045, Val916
10	-7.32	H-bond: Glu885, Asp1046, Cys919. Hydrophobic interaction: Val848, Ala866, Leu840, Leu1035, Val899, Cys1045, Val916
11	-7.94	H-bond: Lys868, Cys919, Val 916. Hydrophobic interaction: Val848, Ala866, Leu840, Leu1035, Val899
13	-10.06	H-Bond: Cys919, Lys868. Hydrophobic interaction: Val848, Ala866, Leu840, Leu1035, Val899, Val914, Val916, Phe1047, Phe 918
Axitinib	-12.78	H-bond: Glu885, Asp1046, Glu917, Cys919. Hydrophobic interaction: Lys868, Val914, Val916, Leu1035, Ala866, Cys1045, Val848, Val899, Phe1047, Phe918, Leu840

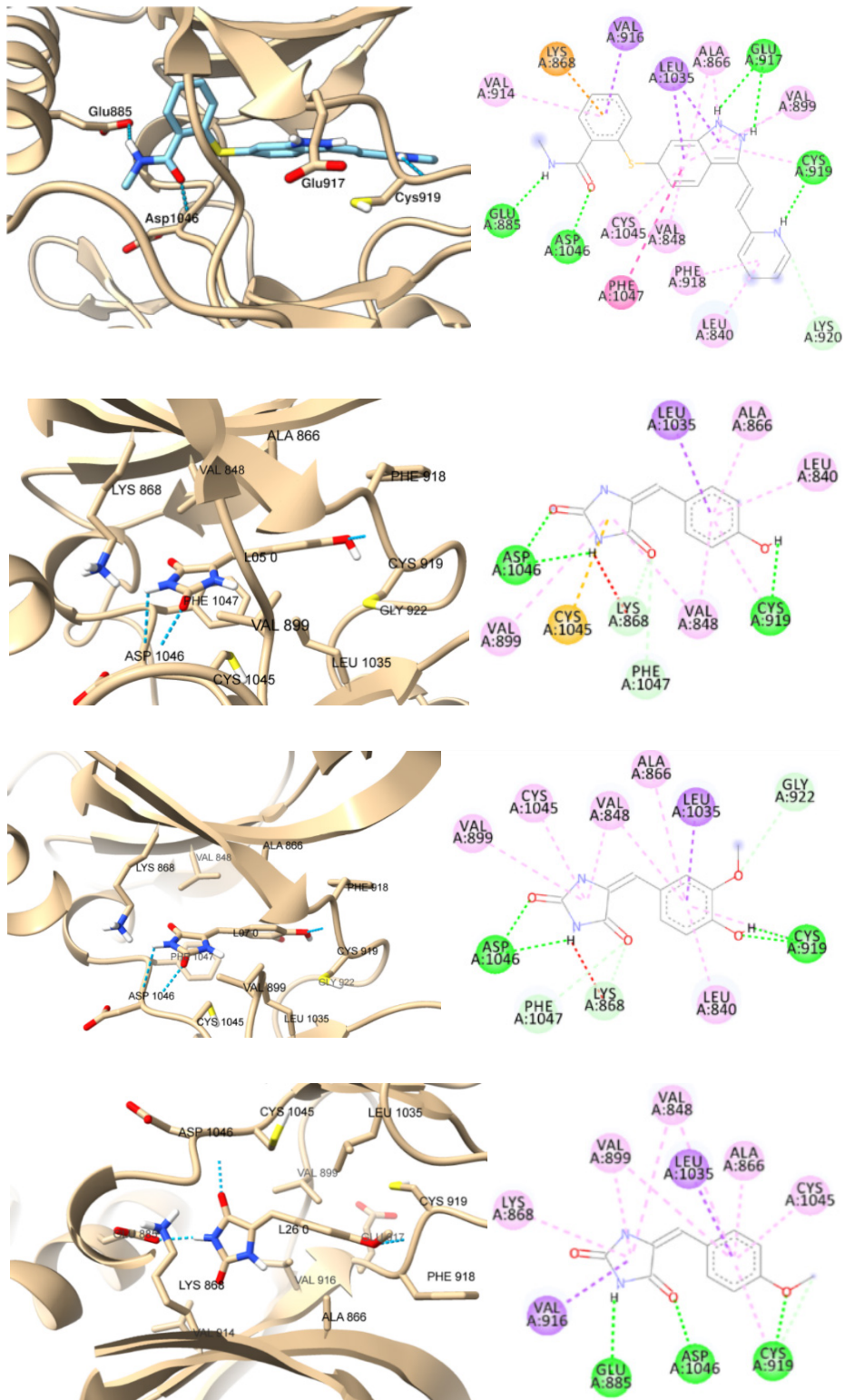


FIGURE 3. Molecular docking visualization of axitinib, **6**, **8**, and **10** in the VEGFR2 catalytic pocket (left = 3D visualization, blue-dashed line = H-bond, right = 2D visualization, green-dashed line = H-bond)

hydantoin's ring resided in the hinge region and formed H-bond with Cys919. In addition, their hydroxyl and methoxy benzylidene moieties formed hydrogen bonds with Glu885 and Asp1046 (Figure 4). While compound **5** has the same pose as **6**, **8**, and **10**, the absence of hydroxy and methoxy groups likely results in the loss of inhibition capability (Figure 5). Moreover, a long alkyl chain at N-3 hydantoin must be avoided since pentyl moiety (compound **11**) created steric hindrance in the allosteric pocket of VEGFR-2 as it showed weaker inhibition activity (Figure 5).

A literature search showed that several synthetic compounds have been reported to have promising VEGFR-2 and related VEGFR inhibitors. It includes indoline, quinoline, pyridine, and pyrimidine derivatives containing one or more *N*-heterocyclic rings (Modi & Kulkarni 2019). The drugs approved as PDGFR inhibitors include imatinib, linifanib, nintedanib, sorafenib, sunitinib, avapritinib, and ripretinib (Kanaan & Strange 2017; Roskoski 2024; Teli & Chawla 2021). These drugs contain one or more *N*-heterocyclic rings. Previously, Carmi et al. (2006) reported that 5-benzylidene-hydantoin could inhibit up to 61% of EGFR autophosphorylation. Further study showed that 5-benzylidene-hydantoin also induced apoptotic cell death (Carmi et al. 2006; Cavazzoni et al. 2008). Sallam et al. (2014) reported that fluoro 5-benzylidene-hydantoin marked a reduction of c-Met kinase level in western blot analysis; this compound also has $IC_{50} = 6.8$ and $3.8 \mu M$, respectively, towards PC-3 and MDA-MB-23. In this study, we reported that compounds **8** and **10** are novel selective

VEGFR-2 and PDGFR inhibitors in which the hydantoin moiety supplies the *N*-heterocyclic ring. The low inhibitory properties of **8** and **10** might be due to the smaller size of the molecules and lack of pharmacophoric features compared to the available drugs for VEGFR-2 and PDGFR inhibitors. Further developments of VEGFR-2 and PDGFR inhibitors based on **8** and **10** structures are thus needed to achieve the IC_{50} values in the range of nanomolar concentrations.

Compounds **8** and **10** structures could be modified into compounds **12** or **13**, incorporating *N*-heterocyclic rings, aromatic linker, urea as hydrogen bond donor and acceptor to DFG motif, and the hydrophobic group (Figure 6). About 14% of approved kinase inhibitors has quinazoline scaffold (Attwood et al. 2021) and it has been observed that the activity and selectivity of VEGFR-2 inhibitions are enhanced when urea and quinazoline are combined (Garofalo et al. 2010; Zayed 2023). Hence, we docked chemical **13** towards the VEGFR-2 ATP binding site because it has a quinazoline ring and a urea-like moiety (hydantoin). Molecular docking of **13** showed that the observed binding affinity is significantly lower than **5-11** (-10.06 kcal/mol vs -6.47 to -7.49 kcal/mol). Compound **13** poses similarly with axitinib (Figure 7); while axitinib's heterocyclic formed a hydrogen bond with Glu917, hydantoin of compound **13** formed a hydrogen bond with Cys919 (Figure 7). Quinazoline of **13** filled the allosteric pocket and formed hydrogen bonding Lys868, and benzylidene moiety of **13** filled the hydrophobic pocket and interacted with Val848, Ala866, and Leu1035 (Figure 7).

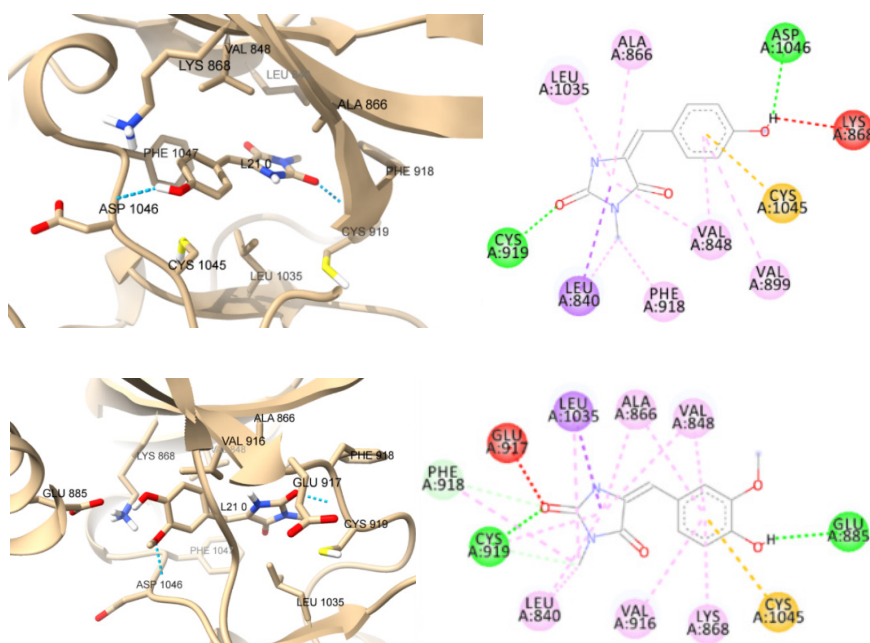


FIGURE 4. Molecular docking visualization of **7** and **9** in the VEGFR2 catalytic pocket (left = 3D visualization, blue-dashed line = H-bond, right = 2D visualization, green-dashed line = H-bond)

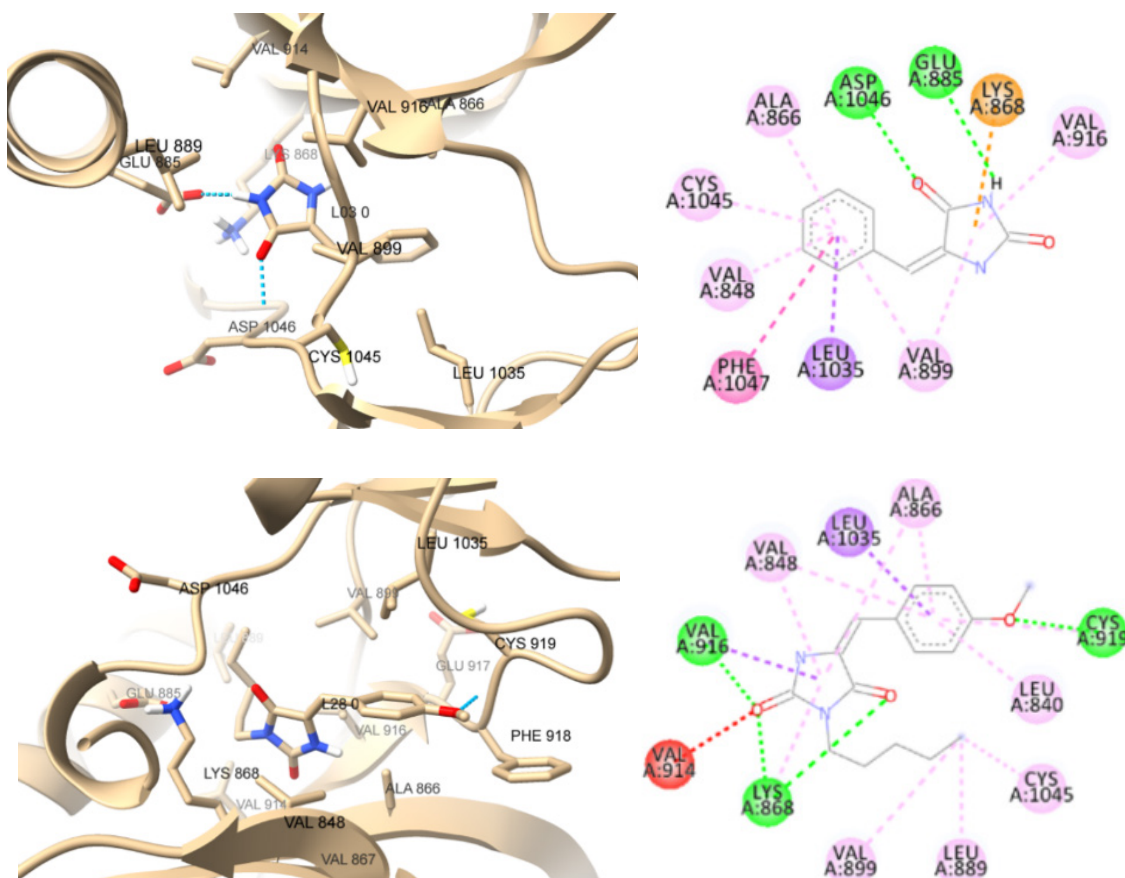


FIGURE 5. Molecular docking visualization of compounds **5** and **11** in the VEGFR2 catalytic pocket (left = 3D visualization, blue-dashed line = H-bond, right = 2D visualization, green-dashed line = H-bond)

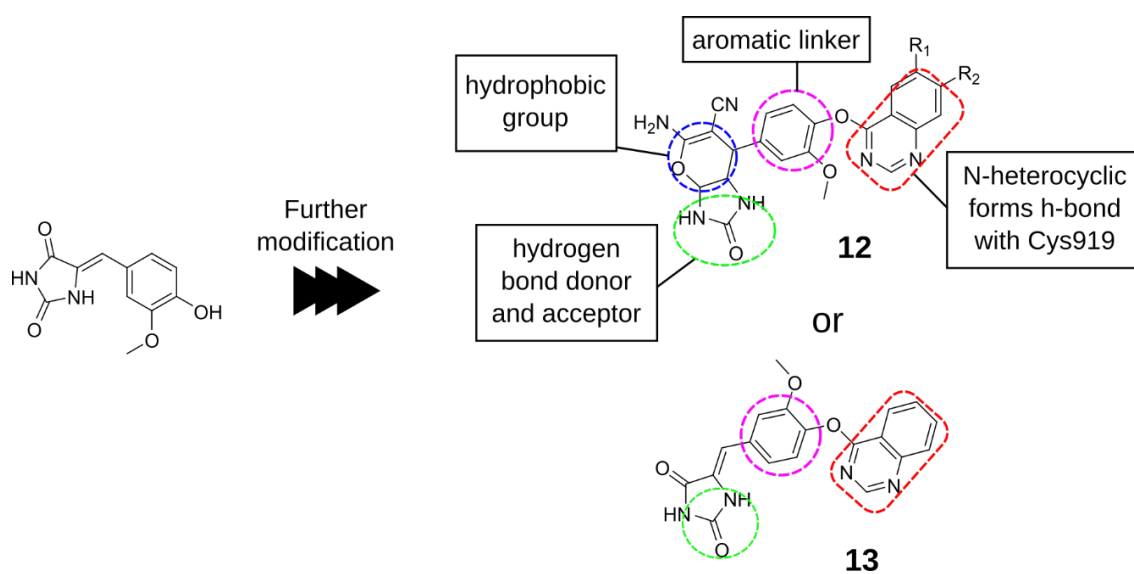


FIGURE 6. Further possible structural improvement of VEGFR-2 inhibitor based on compounds **8** and **10** scaffolds

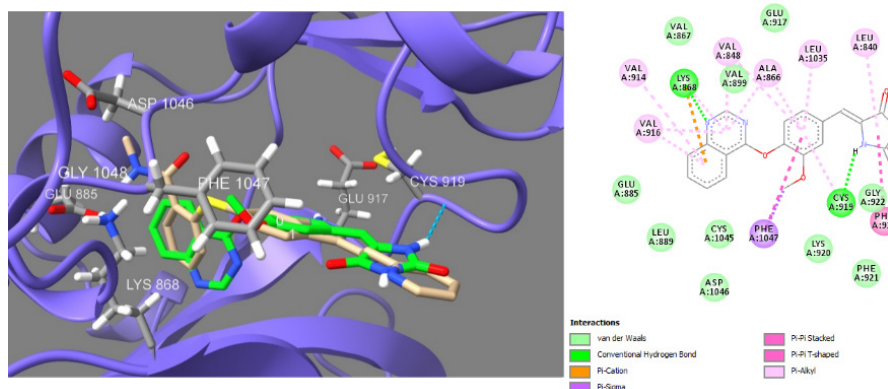


FIGURE 7. Molecular docking visualization of **13** in the VEGFR2 catalytic pocket (left = 3D visualization, blue-dashed line = H-bond, green = compound **13**, cream = axitinib. right = 2D visualization, green-dashed line = H-bond)

CONCLUSION

Using the Knoevenagel condensation and alkylation procedure, two novel benzalhydantoin compounds (**10–11**) have been created from hydantoin and benzaldehyde derivatives, yielding 20 and 17%, respectively. Initial screening evaluation of **5–11** against eight RTKs (EGFR, HER2, HER4, IGF1R, InsR, VEGFR-2, PDGFR- α , and - β) showed that the derivatives **8** and **10** are promising lead compounds for selective VEGFR-2 and PDGFR inhibitors. In addition, docking simulation explained that **5–11** bind into the ATP binding site of VEGFR-2 (PDB ID: 4AG8) and formed a similar interaction in comparison with axitinib. Further investigation of VEGFR-2 and PDGFR inhibitors based on these two compounds (**8** and **10**) would be promising in gaining better activities and a deeper understanding of their mechanisms of action in inhibiting VEGFR-2 and PDGFR.

ACKNOWLEDGEMENTS

The authors are grateful for the financial support from the research grants of PDD, KEMDIKBUDRISTEK (No. 3018/UN6.3.1/PT.00/2023), and PPMI, Institut Teknologi Bandung (No. 93/IT1.C02/SK-TA/2023). We also thank Mrs. Elvira Hermawati, Laboratorium Kimia Terpadu FMIPA-ITB, for recording the NMR data. Molecular graphics and analyses performed with UCSF ChimeraX, developed by the Resource for Biocomputing, Visualization, and Informatics at the University of California, San Francisco, with support from the National Institutes of Health R01-GM129325 and the Office of Cyber Infrastructure and Computational Biology, National Institute of Allergy and Infectious Diseases. This article is dedicated to the late Prof. Yana Maolana Syah.

REFERENCES

- Akeng'a, T.O. & Read, R.W. 2007. Synthesis of imidazol[1,5-a]indole-1,3-diones from imidazolidene-2,4-diones. *South African Journal of Chemistry* 60: 11-16.
- Akeng'a, T.O. & Read, R.W. 2005. Synthesis of indoles: Tetrahydropyrazino[1,2-a]indole-1,4-dione and pyrazino[1,2-a]indole-6,13-diones from piperazine-2,5-diones. *South African Journal of Chemistry* 58: 93-97.
- Attwood, M.M., Fabbro, D., Sokolov, A.V., Knapp, S. & Schiöth, H.B. 2021. Trends in kinase drug discovery: Targets, indications and inhibitor design. *Nature Reviews Drug Discovery* 20(11): 839-861.
- Butti, R., Das, S., Gunasekaran, V.P., Yadav, A.S., Kumar, D. & Kundu, G.C. 2018. Receptor tyrosine kinases (RTKs) in breast cancer: signaling, therapeutic implications and challenges. *Molecular Cancer* 17: 34.
- Carmi, C., Cavazzoni, A., Zuliani, V., Lodola, A., Bordi, F., Plazzi, P.V., Alfieri, R.R., Petronini, P.G. & Mor, M. 2006. 5-Benzylidene-hydantoin as new EGFR inhibitors with antiproliferative activity. *Bioorganic & Medicinal Chemistry Letters* 16(15): 4021-4025.
- Cavazzoni, A., Alfieri, R.R., Carmi, C., Zuliani, V., Galetti, M., Fumarola, C., Frazzi, R., Bonelli, M., Bordi, F., Lodola, A., Mor, M. & Petronini, P.G. 2008. Dual mechanisms of action of the 5-benzylidene-hydantoin UPR1024 on lung cancer cell lines. *Molecular Cancer Therapeutics* 7(2): 361-370.
- Cho, S., Kim, S-H. & Shin, D. 2019. Recent applications of hydantoin and thiohydantoin in medicinal chemistry. *European Journal of Medicinal Chemistry* 164: 517-545.
- Cohen, P. 2002. Protein kinases - the major drug targets of the twenty-first century? *Nature Reviews Drug Discovery* 1(4): 309-315.

- Cohen, P., Cross, D. & Jänne, P.A. 2021. Kinase drug discovery 20 years after imatinib: Progress and future directions. *Nature Reviews Drug Discovery* 20(7): 551-569.
- Dong, Q., Yu, P., Ye, L., Zhang, J., Wang, H., Zou, F., Tian, J. & Kurihara, H. 2019. PCC0208027, a novel tyrosine kinase inhibitor, inhibits tumor growth of NSCLC by targeting EGFR and HER2 aberrations. *Scientific Reports* 9(1): 5692.
- Du, Z. & Lovly, C.M. 2018. Mechanisms of receptor tyrosine kinase activation in cancer. *Molecular Cancer* 17: 58.
- Fischer, A., Smieško, M., Sellner, M. & Lill, M.A. 2021. Decision making in structure-based drug discovery: Visual inspection of docking results. *Journal of Medicinal Chemistry* 64(5): 2489-2500.
- Garofalo, A., Goossens, L., Lemoine, A., Farce, A., Arlot, Y. & Depreux, P. 2010. Quinazoline-urea, new protein kinase inhibitors in treatment of prostate cancer. *Journal of Enzyme Inhibition and Medicinal Chemistry* 25(2): 158-171.
- Hennek, J., Alves, J., Yao, E., Goueli, S.A. & Zegzouti, H. 2016. Bioluminescent kinase strips: A novel approach to targeted and flexible kinase inhibitor profiling. *Analytical Biochemistry* 495: 9-20.
- Hermawati, E., Ellita, S.D., Juliawaty, L.D., Hakim, E.H., Syah, Y.M. & Ishikawa, H. 2020. Epoxyquinophomopsins A and B from endophytic fungus *Phomopsis* sp. and their activity against tyrosine kinase. *Journal of Natural Medicines* 75: 217-222.
- Hidayat, I.W., Sumiarsa, D., Permatasari, M., AKania, Riska & Priani, L. 2017. Synthetic studies of bioactive substances of 4-hydroxybenzalhydantoin derivatives. *IOP Conference Series: Materials Science and Engineering* 172(1): 012024.
- Hidayat, I.W., Thu, Y.Y., Black, D.S.C. & Read, R.W. 2016. Biological evaluation of certain substituted hydantoins and benzalhydantoins against microbes. *IOP Conference Series: Materials Science and Engineering* 107: 012058.
- Horikawa, S., Ishii, Y., Hamashima, T., Yamamoto, S., Mori, H., Fujimori, T., Shen, J., Inoue, R., Nishizono, H., Itoh, H., Majima, M., Abraham, D., Miyawaki, T. & Sasahara, M. 2015. PDGFR α plays a crucial role in connective tissue remodeling. *Scientific Reports* 5(1): 17948.
- Jangir, N., Poonam, Dhadda, S. & Jangid, D.K. 2022. Recent advances in the synthesis of five- and six-membered heterocycles as bioactive skeleton: A concise overview. *ChemistrySelect* 7(6): e202103139.
- Kanaan, R. & Strange, C. 2017. Use of multitarget tyrosine kinase inhibitors to attenuate platelet-derived growth factor signalling in lung disease. *European Respiratory Review* 26(146): 170061.
- Konnert, L., Lamaty, F., Martinez, J. & Colacino, E. 2017. Recent advances in the synthesis of hydantoins: The state of the art of a valuable scaffold. *Chemical Reviews* 117(23): 13757-13809.
- McTigue, M., Murray, B.W., Chen, J.H., Deng, Y-L., Solowiej, J. & Kania, R.S. 2012. Molecular conformations, interactions, and properties associated with drug efficiency and clinical performance among VEGFR TK inhibitors. *Proceedings of the National Academy of Sciences* 109(45): 18281-18289.
- Metibemu, D.S., Akinloye, O.A., Akamo, A.J., Ojo, D.A., Okeowo, O.T. & Omotuyi, I.O. 2019. Exploring receptor tyrosine kinases-inhibitors in cancer treatments. *Egyptian Journal of Medical Human Genetics* 20: 35.
- Modi, S.J. & Kulkarni, V.M. 2019. Vascular endothelial growth factor receptor (VEGFR-2)/KDR inhibitors: Medicinal chemistry perspective. *Medicine in Drug Discovery* 2: 100009.
- Morris, G.M., Huey, R., Lindstrom, W., Sanner, M.F., Belew, R.K., Goodsell, D.S. & Olson, A.J. 2009. AutoDock4 and AutoDockTools4: Automated docking with selective receptor flexibility. *Journal of Computational Chemistry* 30(16): 2785-2791.
- Mudit, M., Khanfar, M., Muralidharan, A., Thomas, S., Shah, G.V., van Soest, R.W.M. & Sayed, K.A.E. 2009. Discovery, design, and synthesis of anti-metastatic lead phenylmethylene hydantoins inspired by marine natural products. *Bioorganic & Medicinal Chemistry* 17(4): 1731-1738.
- Naufal, M., Hermawati, E., Syah, Y.M., Hidayat, A.T., Hidayat, I.W. & Al-Anshori, J. 2024. Structure-activity relationship study and design strategies of hydantoin, thiazolidinedione, and rhodanine-based kinase inhibitors: A two-decade review. *ACS Omega* 9(4): 4186-4209.
- Peng, F-W., Liu, D-K., Zhang, Q-W., Xu, Y-G. & Shi, L. 2017. VEGFR-2 inhibitors and the therapeutic applications thereof: A patent review (2012-2016). *Expert Opinion on Therapeutic Patents* 27(9): 987-1004.
- Pettersen, E.F., Goddard, T.D., Huang, C.C., Meng, E.C., Couch, G.S., Croll, T.I., Morris, J.H. & Ferrin, T.E. 2020. UCSF ChimeraX: Structure visualization for researchers, educators, and developers. *Protein Science* 30(1): 70-82.
- Raap, J., Nieuwenhuis, S., Creemers, A., Hexspoor, S., Kragl, U. & Lugtenburg, J. 1999. Synthesis of isotopically labelled L-phenylalanine and L-tyrosine. *European Journal of Organic Chemistry* 1999(10): 2609-2621.
- Reddy, Y.T., Reddy, P.N., Koduru, S., Damodaran, C. & Crooks, P.A. 2010. Aplysinopsin analogs: Synthesis and anti-proliferative activity of substituted (Z)-5-(N-benzylindol-3-ylmethylene)imidazolidine-2,4-diones. *Bioorganic & Medicinal Chemistry* 18(10): 3570-3574.

- Roskoski, R. 2024. Properties of FDA-approved small molecule protein kinase inhibitors: A 2024 update. *Pharmacological Research* 200: 107059.
- Sallam, A.A., Mohyeldin, M.M., Foudah, A.I., Akl, M.R., Nazzal, S., Meyer, S.A., Liu, Y-Y. & Sayed, K.A.E. 2014. Marine natural products-inspired phenylmethylenedihydantoins with potent *in vitro* and *in vivo* antitumor activities via suppression of Brk and FAK signaling. *Organic and Biomolecular Chemistry* 12(28): 5295-5303.
- Sun, X., Xu, S., Yang, Z., Zheng, P. & Zhu, W. 2020. Epidermal growth factor receptor (EGFR) tyrosine kinase inhibitors for the treatment of non-small cell lung cancer: A patent review (2014-present). *Expert Opinion on Therapeutic Patents* 31(3): 223-238.
- Teli, G. & Chawla, P.A. 2021. Hybridization of imidazole with various heterocycles in targeting cancer: A decade's work. *ChemistrySelect* 6(19): 4803-4836.
- Thenmozhiyal, J.C., Wong, P.T.-H. & Chui, W.-K. 2004. Anticonvulsant activity of phenylmethylenedihydantoins: A structure-activity relationship study. *Journal of Medicinal Chemistry* 47(6): 1527-1535.
- Tirado-Rives, J. & Jorgensen, W.L. 2008. Performance of B3LYP density functional methods for a large set of organic molecules. *Journal of Chemical Theory and Computation* 4(2): 297-306.
- Wang, Z., Sun, H., Yao, X., Li, D., Xu, L., Li, Y., Tian, S. & Hou, T. 2016. Comprehensive evaluation of ten docking programs on a diverse set of protein-ligand complexes: The prediction accuracy of sampling power and scoring power. *Physical Chemistry Chemical Physics* 18(18): 12964-12975.
- Xing, L., Klug-Mcleod, J., Rai, B. & Lunney, E.A. 2015. Kinase hinge binding scaffolds and their hydrogen bond patterns. *Bioorganic & Medicinal Chemistry* 23(19): 6520-6527.
- Yusuf, M., Hardianto, A., Muchtaridi, M., Nuwarda, R.F. & Subroto, T. 2019. Introduction of docking-based virtual screening workflow using desktop personal computer. *Encyclopedia of Bioinformatics and Computational Biology*. Elsevier. pp. 688-699.
- Zayed, M.F. 2023. Medicinal chemistry of quinazolines as anticancer agents targeting tyrosine kinases. *Scientia Pharmaceutica* 91(2): 18.
- Zegzouti, H., Zdanovskaia, M., Hsiao, K. & Goueli, S.A. 2009. ADP-Glo: A bioluminescent and homogeneous ADP monitoring assay for kinases. *ASSAY and Drug Development Technologies* 7(6): 560-572.
- Zhao, Z., Wu, H., Wang, L., Liu, Y., Knapp, S., Liu, Q. & Gray, N.S. 2014. Exploration of Type II binding mode: A privileged approach for kinase inhibitor focused drug discovery? *ACS Chemical Biology* 9(6): 1230-1241.

*Corresponding author; email: jamaludin.al.anshori@unpad.ac.id